RGNZ/MGPB

An Industrial Method for Mitigating Surface Deformations and Restoring Soil Integrity in the Kryvyi Rih Basin

Rudarsko-geološko-naftni zbornik
(The Mining-Geology-Petroleum Engineering Bulletin)
DOI: 10.17794/rgn.2026.1.4

Original scientific paper

Mykhailo Petlovanyi[1], Iryna Fediv[2]*, Vasyl Popovych[2], Taras Boyko[2], Kateryna Stepova[2], Roman Konanets[2], Nataliya Popovych[3]

[1] *Educational and Research Institute of Environmental Management, National Technical University «Dnipro Polytechnic», Dmytro Yavornytskyi Ave. 19, Dnipro, 49005, Ukraine.*

[2] *Faculty of Civil Defence, Lviv State University of Life Safety, Kleparivska Str. 35, Lviv, 79007, Ukraine.*

[3] *Department of Administrative-Legal Disciplines, Lviv State University of Internal Affairs, Gorodotska, 26, 79000, Lviv, Ukraine.*

Abstract

This study addresses the critical issue of technogenic safety and revitalization of devastated landscapes in the Kryvyi Rih basin, a major mining region in Ukraine. It highlights the environmental challenges posed by extensive mining activities, including sinkhole formation, soil degradation, and biodiversity loss, exacerbated by climate change and erosion. The research evaluates the effectiveness of vegetation cover through phytomelioration efficiency coefficients (Kfm), revealing a steady decline from 1984 to 2024 due to expanding devastated areas. For instance, Kfm values dropped from 3.6 to 2.8 for sinkhole No. 1, indicating reduced ecological resilience. A key focus is the proposed cemented paste backfilling technology, utilizing mining waste to fill sinkholes. This method aims to mitigate surface deformations, enhance public safety, and restore soil integrity while repurposing industrial byproducts. The study analyzes sinkhole dynamics using GIS and historical data, identifying nonlinear growth patterns, particularly during 1995–2005. Polynomial models (R^2 up to 0.997) effectively describe these trends. Economic analysis underscores the escalating costs of delayed revitalization, with expenses rising up to sevenfold over 38 years. The research advocates for timely intervention to reduce both environmental risks and financial burdens. In conclusion, the integration of backfilling technologies and phytomelioration strategies offers a sustainable solution for restoring Kryvyi Rih's landscapes, aligning with global climate goals and regional development needs. The findings emphasize the urgency of implementing these measures to ensure ecological stability and long-term socio-economic benefits.

Keywords:
technogenic safety; landscape revitalization; sinkhole remediation; phytomelioration coefficient; mining waste reclamation

1. Introduction

The issues of technogenic safety and the revitalization of devastated landscapes are becoming particularly relevant in the modern world, amid global climate change and growing awareness of environmental issues. The decisions made at the UN Climate Change Conference (COP26) in Glasgow in 2021, as well as at the Paris Climate Summit in 2015, set the global course for reducing greenhouse gas emissions and gradually phasing out fossil fuels. The Paris Agreement laid the groundwork for international cooperation in the field of sustainable development, which involves not only reducing dependence on coal but also active reclamation of devastated areas. By joining these global initiatives, Ukraine has committed itself to reducing emissions and closing state coal-fired power plants (**Cabinet of Ministers of Ukraine, 2013**). However, the process of abandoning the coal industry is inextricably linked to the need to address issues related to large-scale areas devastated by mining activities and the accumulation of significant amounts of industrial waste.

The Kryvyi Rih mining region represents a distinct natural–man-made geosystem, where over a century of intensive iron-ore mining has caused irreversible transformations in both surface and subsurface environments. These activities have disrupted fault-block tectonics and increased neotectonic activity and massif instability (**Evtekhov et al., 2022**).

Large-scale surface deformations have become a defining feature of the Kryvyi Rih Iron Ore basin due to over a century of intensive underground and open-pit mining. Subsidence, sinkholes, and landslide-prone zones currently affect both industrial facilities and residential areas. These processes pose a serious threat to geotechnical stability, public safety, and sustainable land

* Corresponding author: Iryna Fediv
e-mail address: ira.arnaut94@gmail.com
Received: 29 April 2025. Accepted: 14 July 2025.
Available online: 2 January 2026

use. According to recent studies, the deformation zones in Kryvbas cover hundreds of hectares and are expanding annually, particularly in areas of delayed reclamation and insufficient backfilling (**Hubina & Zaborovsky, 2022; Bazaluk et al., 2024**). Therefore, a detailed investigation of their spatial structure, genesis, and mitigation is critically important for regional risk management and engineering planning.

The geomorphological structure of the region has been significantly altered due to open-pit operations, underground cavities, and extensive waste deposition. The territory now features quarries up to 400 m deep, over 4.5 billion m³ of excavated voids, and up to 4,000 ha of subsidence zones and sinkholes. These factors have also reshaped drainage networks and contributed to erosion, karst processes, and surface deformation (**Bazaluk et al., 2024**).

Consequently, the Kryvyi Rih basin has transformed into a complex technogenic geosystem, which requires an integrated approach combining ecological restoration with geotechnical stabilization measures (**Bazaluk et al., 2024**).

The issue of technogenic load is particularly acute for Ukraine, which has a significant mining sector. The accumulated billions of tons of waste, most of which is generated by the mining, chemical and energy sectors, pose serious environmental challenges. Such wastes include coal mining dumps, ore tailings, thermal power plant slag, and others characterized by large volumes and potential environmental hazards (**Pactwa et al., 2020**). These factors necessitate the development and implementation of effective strategies for the revitalization of devastated landscapes, especially in regions of intensive mining activity, such as the Kryvyi Rih basin. A comprehensive environmental policy framework and the evolution of environmental management concepts play a critical role in shaping such strategies (**Hren et al., 2021; Batyr et al., 2021**). Insight from other devastated regions of Ukraine, such as the Volhynian Upland and Male Polissia, demonstrates the broad-scale impact of mining activities and supports the need for adaptive restoration strategies (**Popovych & Voloshchyshyn, 2019**). Valuable insight can be gained from research focused on mining regions across Ukraine, where ecological and phytogenic restoration efforts have been tested on coal mine tailings and waste dumps (**Skrobala et al., 2020; Popovych et al., 2021**). Environmental degradation in post-mining areas may also contribute to increased incidence of chronic diseases, particularly cardiovascular and metabolic disorders (**Serhiyenko & Serhiyenko, 2022**).

The Kryvyi Rih basin, as one of the largest mining regions in Ukraine, is characterized by a significant anthropogenic load and large areas of devastated landscapes. The issue of anthropogenic safety of these areas and their effective revitalization is extremely important for ensuring the environmental safety of the region and sustainable development. Solving this problem requires an integrated approach that combines the analysis of existing anthropogenic risks, the development of effective revitalization methods based on international experience, including the application of geomorphic reclamation techniques (USA), phytoremediation and soil amendment practices (Germany), and cemented paste backfilling technologies (Canada and Australia). These internationally recognized methods are designed to restore land stability, improve soil fertility, and promote biodiversity by reshaping natural landforms, introducing native vegetation, and sustainably reusing mining by-products (**Maiti & Ahirwal, 2019**). The introduction of such technologies is essential for reducing the anthropogenic load and restoring the natural potential of devastated areas. In this context, modelling approaches to predict pollution dynamics in mining regions also play a crucial role in strategic planning (**Pukish et al., 2024**).

The scientific literature focuses on the issues of mining waste management, reclamation of disturbed lands and ecosystem restoration. The research covers a wide range of topics, from geochemical modelling of rock weathering processes (**Strömberg & Banwart, 1994**) and analysis of the current state of coal industry waste (**Gorman & Dzombak, 2018**) to the development of sustainable coal mining strategies (**Kariuki & Kuria, 2021**) and methods of ecological restoration (**Maiti & Ahirwal, 2019**). Research on the reuse and recycling of mine waste, monitoring of mine dumps (**Agboola et al., 2020**), and multi-element geochemical analysis of technologically loaded areas (**Loredo et al., 2006**) are of particular interest.

Recent studies from other European mining regions have also addressed similar challenges, including land destabilization, ineffective mine void management, and long-term ecological risks associated with abandoned extraction areas. These works emphasize the relevance of integrated rehabilitation strategies and underline the importance of biodiversity-oriented reclamation, sustainable reuse of mining waste, and prevention of technogenic hazards (**Bujok et al., 2015; Popovych et al., 2024; Nouri Qarahasanlou et al., 2022; Neral et al., 2023**).

1.1. Geological features of the research area

The territory of Kryvyi Rih district is located within the East European polygenic plain (morphostructure of the first order), which is formed by a large tectonic structure - the East European platform.

The basis of the morphostructural relief of the region is made up of watershed forest plateaus and their slopes, which extend from north and northeast to south, having a general slope towards the Black Sea, as well as towards river valleys and gullies. The watershed plateaus are alignment surfaces of different ages: from residual Late Sarmatian in the north to Pontic in the south. Absolute elevations of the watershed plateau vary from +169-

173 m in the north to +75 m in the south. The decrease in the watershed height in the southern direction is 0.69 m/km. The steepness of the watershed plateaus ranges from 0 to 1.5°, and on the slopes - up to 3-6°. The average density of the horizontal division of the Kryvbas territory by the erosion network is high and ranges from 0.8 to 1.6 km/km. The incision of river valleys relative to the watersheds reaches 70–90 m, and the depth of the gully incision is 20–40 m. These parameters reflect intense fluvial and erosion processes typical for heavily anthropogenically transformed territories. Recent studies confirm that ongoing mining operations have intensified geomorphological fragmentation and landscape instability in the Kryvyi Rih region, resulting in progressive denudation and structural weakening of the surface (**Bazaluk et al., 2024; Evtekhov et al., 2022**).

Geologically, the Kryvyi Rih basin is located in the central part of the Ukrainian crystalline massif and is part of the Kryvyi Rih-Kremenchuk structure and facies zone. The metamorphic rocks of the Kryvyi Rih series that contribute to the formation of the basin stretch in a narrow strip from the InGZK open pit in the south to the Zhovtorichinske deposit in the north, with a total length of over 140 km. Large massifs of granite are developed to the east of this strip, and migmatites to the west. The metamorphic rocks of the Kryvyi Rih series are overlain by sedimentary deposits (sands, clays, limestones, loams), which vary in thickness from 0.5 to 70-80 m (on average 20-30 m).

The rocks of the Kryvyi Rih series are divided into five formations: the novokryvorizka (nk), skelevatska (sk), saxahanska (sx), gdantsivska (gd) and gleyuvatska (gl). The novokryvorizhska suite is represented by amphibolites, while the skelevatska suite is composed of arkose sandstones, phyllites, and talc-carbonate shales. The saksahanska suite is characterized by the alternation of seven ferruginous and seven shale horizons, with some horizons being faulted or cut by tectonic faults.

The morphosculptural relief of the Kryvyi Rih basin was formed under the influence of exogenous geomorphological processes, including fluvial (erosion, washout, sediment transport), gravitational (landslides, collapse) karstic (dissolution of carbonate rocks), sufosic (leaching of fine fractions by groundwater), aeolian (dispersal of alluvial sands), and anthropogenic factors (mining, waste storage) (**Kazakov et al, 2005**).

The city of Kryvyi Rih was formed around the iron ore industry and stretches northeastward along ore deposits (Map of Zoning of the City Territory by Mining and Geological Conditions). The region hosts a powerful metallurgical complex, including ArcelorMittal Kryvyi Rih, with a full cycle of ore processing. These facilities, along with coal- and gas-powered thermal stations, form an energy-intensive system that significantly contributes to local pollution and technogenic pressure (**Bazaluk et al., 2024; Batyr et al., 2021**). Both open and underground mining methods are used in the city. Significant areas of development are excluded from exploitation due to the presence of quarries, dumps, and earth movement zones (**Kryvbassproekt, 2011**).

The subsoil of Kryvbas contains about 30 billion tons of iron ore at depths of 1500-2600 meters. The balance reserves within quarries and mines amount to 6 billion tons, which is 20% of the total reserves. The remaining iron ore reserves are located in the sides of quarries, below the design depth of operating mines, and under built-up areas, which complicates their development and creates potential threats to the environment and the population (**Kazakov et al., 2005**).

2. Methods

2.1. Object discription

The research paper investigates a complex of formed and closely spaced sinkholes, the voids of which are the highest priority for cemented paste backfill (see **Figure 1**), and the conceptual scheme of the backfill technology for better understanding is shown in **Figure 14**. These sinkholes have formed as a result of both natural and anthropogenic processes typical of the Kryvyi Rih mining region. Extensive underground mining without subsequent backfilling has led to the gradual collapse of rock masses and the formation of subsurface voids. Additionally, natural factors such as groundwater leaching (suffosion), karst processes, and neotectonic activity further destabilize the geological environment, accelerating the development of cracks and surface deformations (**Hubina & Zaborovsky, 2022; Kazakov et al., 2005**).

The spatial boundaries of the sinkholes were digitized using time-series satellite imagery (Google Earth Pro, 1984–2024) and topographic plans. Analytical tools included polygon vectorization, area calculations, and change detection using GIS-based measurements. Biodiversity assessment was performed using the phytomelioration coefficient, which serves as an integral indicator of vegetative cover transformation and ecological succession on disturbed lands.

The combination of these influences poses serious threats to the safety of surrounding infrastructure and ecosystems, necessitating timely and effective mitigation measures. Formation of monolithic backfill in the sinkhole zones will allow solving a number of engineering and environmental problems

- reduce the dynamics of deformation processes of the earth's surface around the sinkholes,
- increase safety for life and health of the population;
- prevent further destruction of infrastructure facilities;
- prevent further destruction of valuable soils;
- preserve biocenoses as a result of soil destruction;
- utilize certain volumes of accumulated tailings;
- improve ventilation and drainage of mines by blocking the dip zones with backfill.

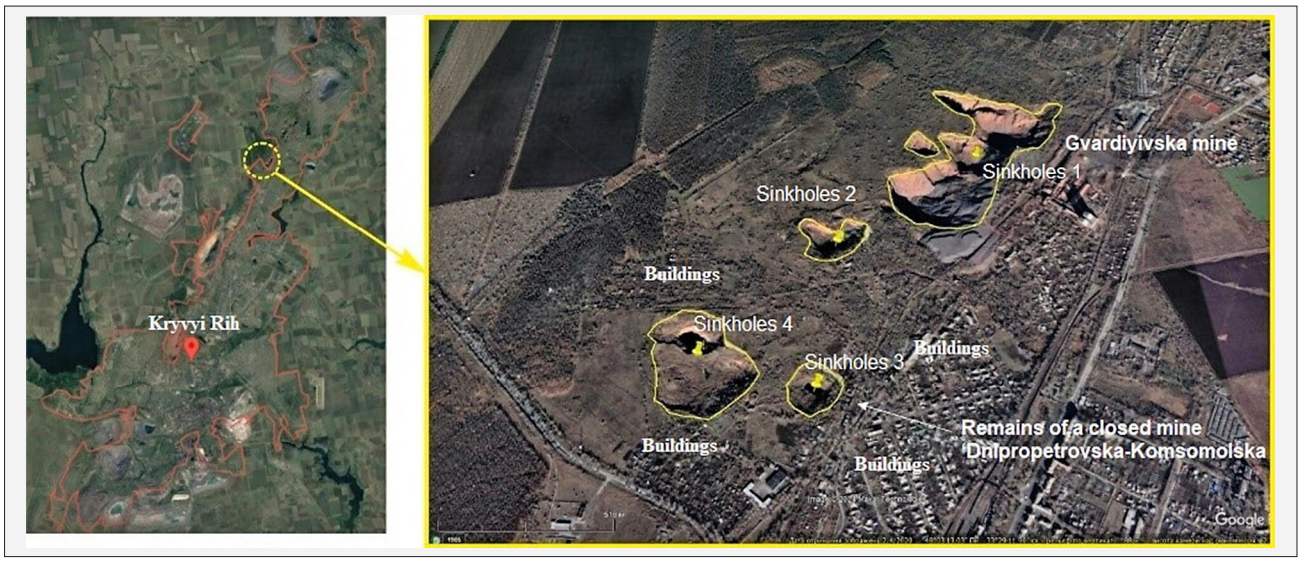

Figure 1. Location of the priority sinkholes on the northwestern outskirts of Kryvyi Rih (coordinates: 48.0668, 33.4052)

In addition to ecological assessments, a technical solution based on cemented paste backfilling was developed and is presented in the Results section as a recommendation for the remediation of sinkhole-affected areas.

2.2. Determination of coefficient of phytomeliorative efficiency

An important aspect of assessing the condition of the research region is the analysis of the vegetation cover, since it is known for its important soil-strengthening role, which is crucial in the context of intensified landslide processes around the studied sinkholes, and reduces the intensity of water and wind erosion. The formation of vegetation cover is important for the succession stages of phytomelioration processes, as an element of improving the mechanical structure of the soil, gradually increasing its fertility.

In this context, the presence and proportion (in %) of different groups of plantations differentiated by their functional purpose was studied. The current state and typology of the vegetation cover of the slopes of these four sinkholes were assessed both in the zone of active development of karst processes and in the adjacent territory that is potentially sinkhole. We also analyzed the dynamics of vegetation change from 1984 to 2024.

A number of trial areas were laid out to analyze the current phytomelioration process taking place in the studied areas of sinkholes, where the coefficient of phytomelioration efficiency of vegetation cover was calculated and evaluated in points.

To determine the coefficient of phytomeliorative efficiency, a generally accepted **Equation 1** was used (**Kucheriavyy, 2003**):

$$K_{FM} = \frac{(S_p \cdot b + S_a \cdot b + S_{pm} \cdot b + S_f \cdot b + S_v \cdot b + S_{sv1} \cdot b + S_{sv2} \cdot b + S_{st} \cdot b + S_r \cdot b)}{S} \quad (1)$$

Where:

S – the area occupied by: S_p - pratocenosis;
S_a – agrocenosis;
S_{pm} – pomolohocenosis;
S_f – frutocenosis;
S_v – vitocenosis;
S_{sv1} – single-tier silvacenosis;
S_{sv2} – two-tiered silvacenosis;
S_{st} – streptocenosis;
S_r – ruderocenosis;
b – the number of points received by the cenosis;
S – total area.

The following differentiation is distinguished according to the functions and possibilities of development in specific conditions of the territory (present or not), of each of the listed groups of plantations: **pratocenoses** - meadow communities, **agrocenoses** - agricultural plantations, **pomolohocenoses** - orchards or their remains, **frutocenoses** - shrub plantations, **vitocenoses** - vineyards, **silvacenoses** - forest communities, **striocenoses** - strips of various functional adaptations, and **ruderalenoses** - weed communities.

3. Results and Discussion

3.1. Spatiotemporal Dynamics of Sinkhole Expansion

The sinkholes are expanding over time, which is likely caused by two factors:

- further increase in the depth of ore reserves in existing mines and the gradual continuation of landslide processes in the mountain massif;
- the impact of climatic factors, water and wind erosion, which causes soil layers to collapse into space (similar to the principle of ravine expansion).

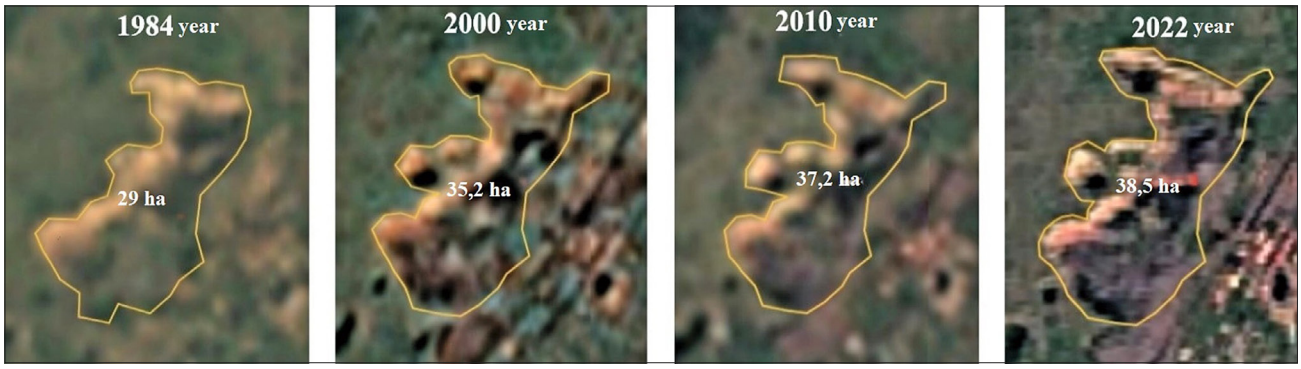

Figure 2. Historical dynamics of the disturbed earth surface area of sinkhole 1 (coordinates: 48.0639, 33.4831)

These 4 dip zones of the earth's surface were selected for backfilling because of their shortest distance to the tailings pond as a source of the main component of paste backfilling - fine iron ore tailings. A relatively short distance of 4-5 km from the tailings dump to the dip zones creates conditions for filling their voids with cemented paste backfill.

Figure 1 illustrates the location of the sinkholes. It should be noted that the sinkholes were formed as a result of iron ore mining without underground sealing technologies in both operating mines and mines that were closed long ago (1930-1950). Therefore, the dynamics of the increase in the area of sinkholes may differ. If a mine has been closed for a long time, the development of massif deformations is relatively stabilized and the expansion of sinkholes is mainly influenced by climatic factors. If the mine is active, the intensity of deformation of the massif is greater, although it is also slightly stabilized in time and the influence of climatic factors is also included.

Establishing the affiliation of sinkholes to specific mines is complicated, since many mines, including shallow ones, operated in the 20th century. Documentation of mining plans for many closed mines was lost during the Second World War. Therefore, data from various information sources are used to establish the approximate location.

In **Figure 1**, sinkholes 1, 2 were formed as a result of the extraction of iron ore reserves at the Hvardiyska mine, which is still in operation. Sinkholes 3, 4 were probably formed as a result of ore mining at the closed Dnipropetrovska-Komsomolska mine.

Photos of sinkholes 1-4 are shown in **Figures 10-11**. It should be noted that the earth's surface deformations can be represented by two forms - zones of smooth lowering and sinkholes, which is well illustrated by the example of sinkhole 4 (see **Figure 5**).

The approximate dynamics of the development of the area of earth surface disturbance around the sinkholes was estimated using the function of viewing historical images in the web version of the Google Earth service. Historical images of sinkholes 1-4 from 1984 to 2024 were analyzed. An example of the historical dynamics of the disturbed earth surface area is shown on the example of sinkhole 1 (see **Figure 2**).

The quantitative dynamics of changes in the disturbed area of the earth's surface is shown in **Figures 3-6**.

The analysis of **Figures 3-6** shows that the increase in the area of sinkholes may have different dynamics. Thus, as of 1984, sinkholes 1-4 were already partially formed and increased in the area of the disturbed surface in time until 2024. Sinkholes 1 and 2 have changed gradually over time and probably indicate that the maximum intensity of landslide geomechanical processes in the mas-

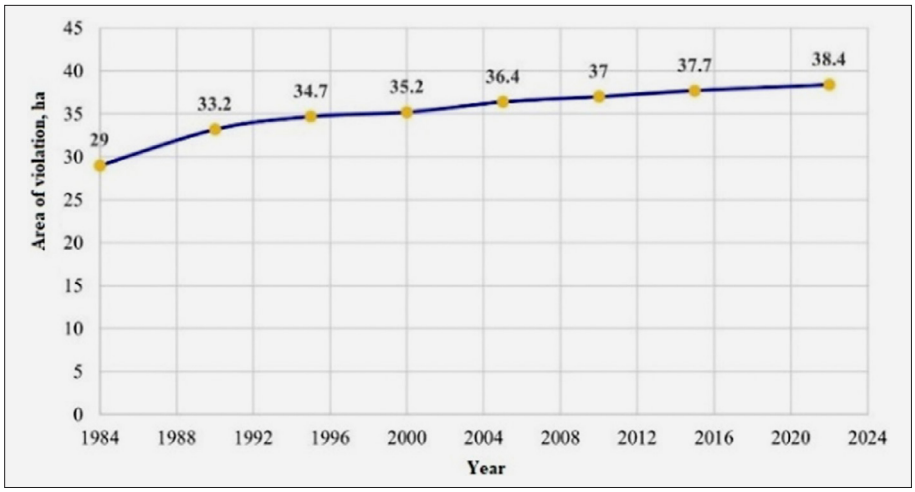

Figure 3. Dynamics of changes in the area of the disturbed earth surface of sinkhole 1

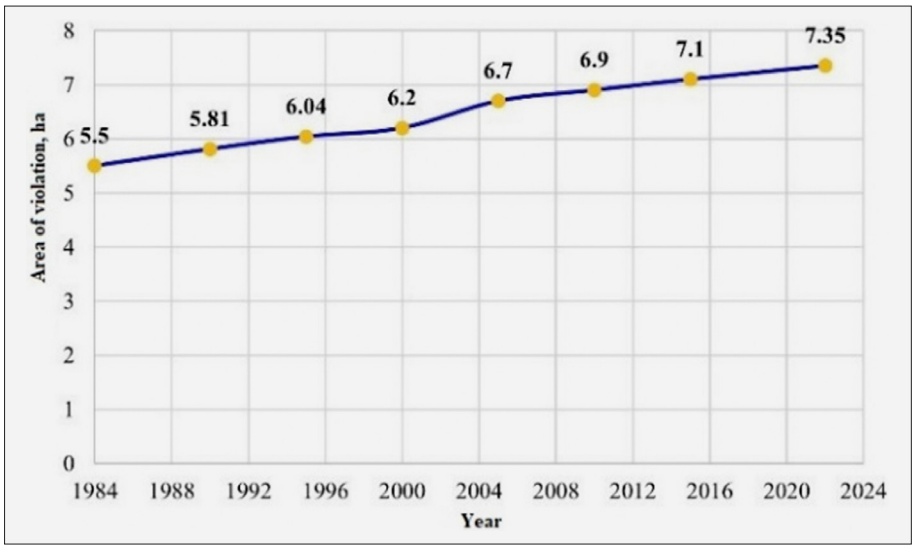

Figure 4. Dynamics of changes in the area of the disturbed earth surface of sinkhole 2

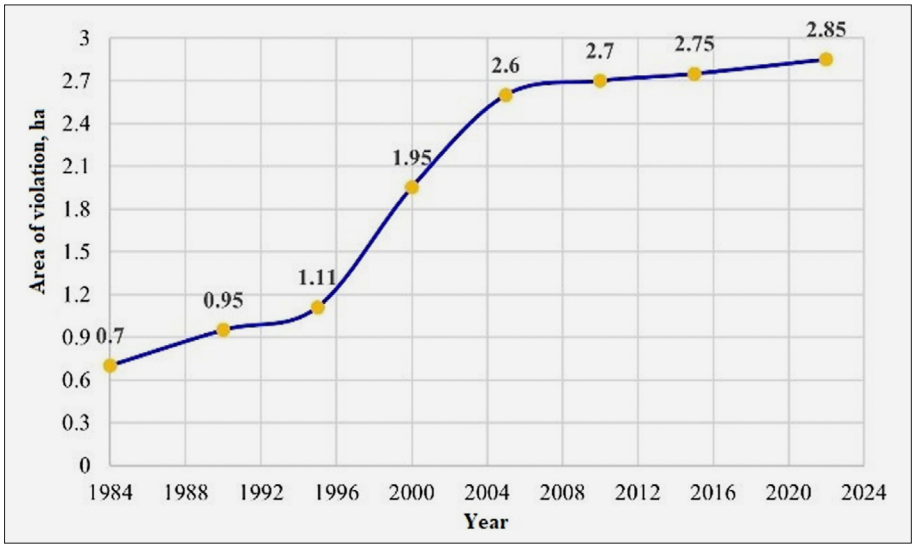

Figure 5. Dynamics of changes in the area of the disturbed earth surface of sinkhole 3

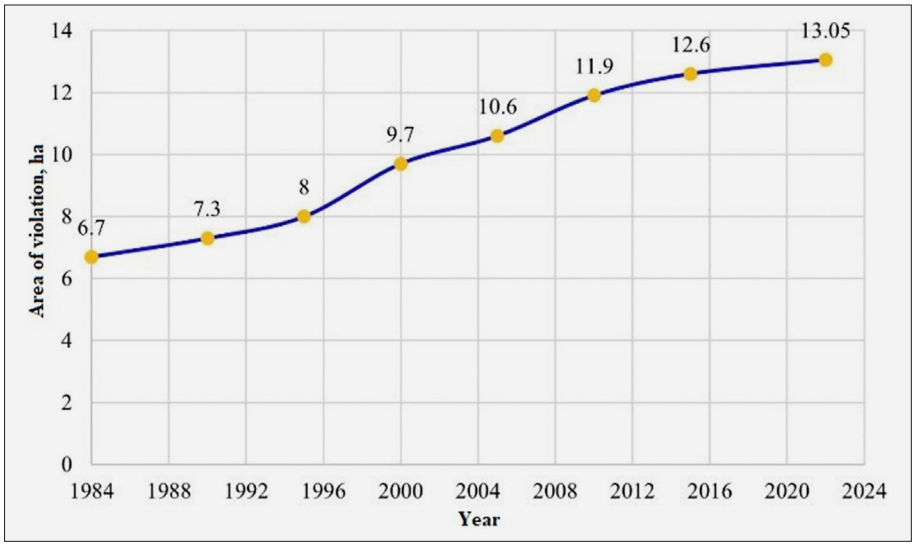

Figure 6. Dynamics of changes in the area of the disturbed earth surface of sinkhole 4

sif occurred earlier, before 1984, and further the area increase is gradual, mainly due to the influence of erosion processes and insignificant intensity of landslide processes. The area of sinkholes 3 and 4 changed most intensively from 1995 to 2005. Probably, during this period there was a peak of landslide geomechanical processes in the massif, and since 2005 the dynamics of the area expansion has significantly decreased and is probably due to the influence of erosion processes and low intensity of landslide processes.

The evolution of the sinkhole area, proven by GIS observations, threatens the safety of the people living in nearby villages, destroys infrastructure, degrades soil cover, and reduces biodiversity, which is a serious technogenic and environmental problem. The development of sinkholes is uncontrollable and unpredictable, and their intensity depends on a number of factors. The monolithic filling of sinkholes may create a "sealing" effect and prevent further increase in their area. This effect is achieved by injecting a cemented paste backfill composed of fine iron ore tailings, Portland cement, blast furnace slag, and fly ash. The paste is prepared in a mobile mixing unit and delivered under pressure through a pipeline network into the sinkhole voids. Once hardened, the mixture forms a dense, water-resistant mass that stabilizes the surrounding rock massif and minimizes further surface deformation. According to field studies, such backfills demonstrate compressive strength exceeding 2.5–3.0 MPa, with an estimated sealing effectiveness lasting over 20–30 years, depending on local hydrogeological conditions (**Hubina & Zaborovsky, 2022**).

The cemented paste backfilling (CPB) mixture was developed using a combination of iron ore tailings (60–65%), blast furnace slag (15–20%), Portland cement (10–12%), and water (10–12%). The mixture was prepared in mobile mixing units and transported to the sinkhole via a high-pressure pump and pipeline system. Upon filling, the paste hardens into a monolithic structure with compressive strength exceeding 2.5–3.0 MPa within 28 days. This method ensures long-term stabilization of subsurface voids and reduces surface deformation risks. For detailed technical implementation, readers are referred to **Hubina & Zaborovsky (2022)**.

3.2. Ecological features of vegetation cover

In the structure of the identified woody and herbaceous species, the following groups were distinguished with regard to habitat richness: species that prefer medium trophic habitat conditions (mesotrophs), species that prefer rich habitat conditions (eutrophs), and species that prefer poor habitat conditions (oligotrophs). The distribution of these groups is shown below (see **Figure 7**).

Thus, the proportion of oligotrophs growing on poor soils is 46%, mesotrophs preferring average soil fertility conditions is 48%, and eutrophs preferring fertile habitat conditions is only 6%.

According to the indicator of the substrate moisture content, a number of classification groups are distinguished, namely: mesocerophytes - plants adapted to conditions slightly less than average for soil moisture reserves; mesophytes - species that prefer medium moisture conditions and hygrophytes - those that prefer moist habitats (see **Figure 8**).

The mesophyte group is the most represented - 47%, followed by mesocerophytes - 50% and hygrophytes - 3%.

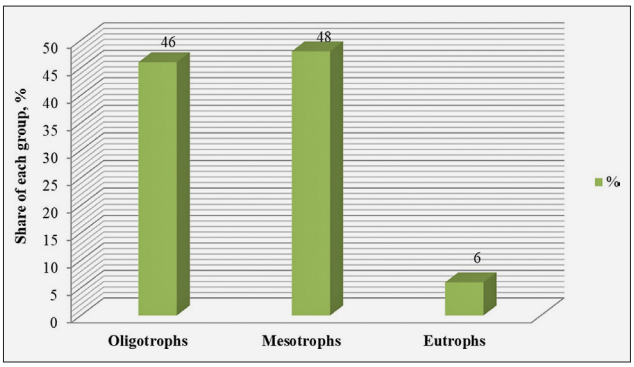

Figure 7. Vegetation structure by trophomorphs

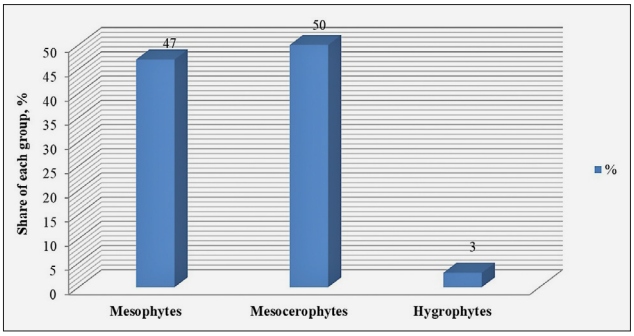

Figure 8. Vegetation structure by hydromorphs

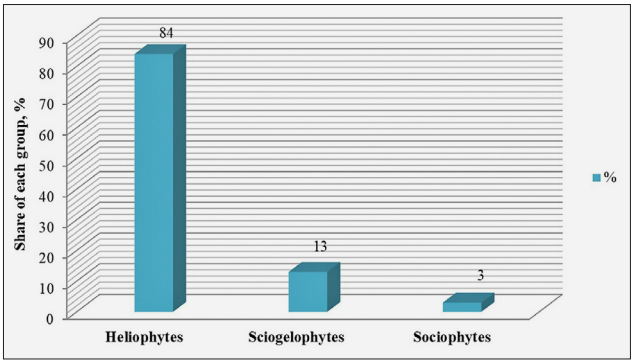

Figure 9. Vegetation structure by heliomorphs

The following groups were identified in relation to lighting: sociophytes, species that are shade-loving, sociogeliophytes - shade-tolerant species, and heliophytes that prefer open habitats with significant light. Their distribution is shown below (see **Figure 9**).

Among the species that form the vegetation cover of the study area, heliophytes dominate (84%), sociogeliofes - 13%, and sociophytes - 3%.

3.3. Coefficient of phytomelioration efficiency

Depending on the identified groups of plantations, the structure of the basic equation (**Equations 2-17**) changes in different study periods.

The following phytoreclamation groups of plantations were identified as a result of the research:

Figure 10. Sinkhole No. 1 (photo by Dmitry Antonov, 2015)

2024: pratocenosis (S_p) – 40%, ruderocenosis (S_r.) – 10%, single-tier silvacenosis (S_{sv1}) – 15%, terrain without vegetation – 35%.

The equation for the phytomelioration activity coefficient is as follows:

$$K_{FM} = \frac{S_{sv1\times b+S_r\times b+}S_{p\times b}}{s} \quad (2)$$

2010: pratocenosis (S_p) – 45%, ruderocenosis (S_r.) – 7%, single-tier silvacenosis (S_{sv1}) – 18%, frutocenosis (S_f) – 5%, terrain without vegetation– 25%.

The equation for the phytomelioration activity coefficient is as follows:

$$K_{FM} = \frac{S_{sv1\times b+S_f\times b+}S_{p\times b+S_{r\times b}}}{s} \quad (3)$$

2000: pratocenosis (S_p) – 48%, ruderocenosis (S_r.) – 5%, single-tier silvacenosis (S_{sv1}) – 20%, frutocenosis (S_f) – 5%, terrain without vegetation – 22%.

The equation for the phytomelioration activity coefficient is as follows:

$$K_{FM} = \frac{S_{sv1\times b+S_f\times b+}S_{p\times b+S_{r\times b}}}{s} \quad (4)$$

1984: pratocenosis (S_p) – 50%, ruderocenosis (S_r.) – 3%, single-tier silvacenosis (S_{sv1}) – 22%, two-tiered silvacenosis (S_{sv2}) – 3%, frutocenosis (S_f) – 10%, terrain without vegetation – 12%.

The equation for the phytomelioration activity coefficient is as follows:

$$K_{FM} = \frac{S_{sv1\times b+Ssv2\times b+S_f\times b+}S_{p\times b+S_{r\times b}}}{s} \quad (5)$$

Figure 11. Sinkhole No. 2
(photo by Dmitry Antonov, 2015)

The following ratio of phytomelioration groups of plantations was established as a result of the research:

2024: pratocenosis (S_p) – 44%, ruderocenosis (S_r.) – 13%, single-tier silvacenosis (S_{sv1}) – 12%, terrain without vegetation – 31%.

The equation for the phytomelioration activity coefficient is as follows:

$$K_{FM} = \frac{S_{sv1\times b+S_r\times b+}S_{p\times b}}{s} \quad (6)$$

2010: pratocenosis (S_p) – 47%, ruderocenosis (S_r.) – 9%, single-tier silvacenosis (S_{sv1}) – 20%, terrain without vegetation – 24%.

The equation for the phytomelioration activity coefficient is as follows:

$$K_{FM} = \frac{S_{sv1\times b+S_r\times b+}S_{p\times b}}{s} \quad (7)$$

2000: pratocenosis (S_p) – 50%, ruderocenosis (S_r.) – 4%, single-tier silvacenosis (S_{sv1}) – 23%, frutocenosis (S_f) – 6%, terrain without vegetation – 17%.

The equation for the phytomelioration activity coefficient is as follows:

$$K_{FM} = \frac{S_{sv1\times b+S_f\times b+}S_{p\times b+S_{r\times b}}}{s} \quad (8)$$

1984: pratocenosis (S_p) – 53%, ruderocenosis (S_r.) – 2%, single-tier silvacenosis (S_{sv1}) – 25%, frutocenosis (S_f) – 10%, terrain without vegetation – 10%.

The equation for the phytomelioration activity coefficient is as follows:

$$K_{FM} = \frac{S_{sv1\times b+S_f\times b+}S_{p\times b+S_{r\times b}}}{s} \quad (9)$$

The following ratio of phytomeliorative plantation groups was established at this site:

2024: pratocenosis (S_p) – 41%, ruderocenosis (S_r.) – 18%, single-tier silvacenosis (S_{sv1}) – 12%, terrain without vegetation – 29%.

The equation for the phytomelioration activity coefficient is as follows:

$$K_{FM} = \frac{S_{sv1\times b+S_r\times b+}S_{p\times b}}{s} \quad (10)$$

Figure 12. Sinkhole No. 3 (photo by Dmitry Antonov, 2015)

Figure 13. Sinkhole No. 4 (photo by Dmitry Antonov, 2015)

2010: pratocenosis (S_p) – 45%, ruderocenosis (S_r.) – 11%, single-tier silvacenosis (S_{sv1}) – 22%, terrain without vegetation – 22%.

The equation for the phytomelioration activity coefficient is as follows:

$$K_{FM} = \frac{S_{sv1\times b+S_r\times b+S_{p\times b}}}{s} \quad (11)$$

2000: pratocenosis (S_p) – 48%, ruderocenosis (S_r.) – 2%, single-tier silvacenosis (S_{sv1}) – 26%, frutocenosis (S_f) – 7%, terrain without vegetation – 17%.

The equation for the phytomelioration activity coefficient is as follows:

$$K_{FM} = \frac{S_{sv1\times b+S_f\times b+S_{p\times b+S_{r\times b}}}}{s} \quad (12)$$

1984: pratocenosis (S_p) – 50%, ruderocenosis (S_r.) – 2%, single-tier silvacenosis (S_{sv1}) – 27%, two-tiered silvacenosis (S_{sv2}) – 3%, frutocenosis (S_f) – 9%, terrain without vegetation – 9%.

The equation for the phytomelioration activity coefficient is as follows:

$$K_{FM} = \frac{S_{sv1\times b+Ssv2\times b+S_f\times b+S_{p\times b+S_{r\times b}}}}{s} \quad (13)$$

2024: pratocenosis (S_p) – 37%, ruderocenosis (S_r.) – 11%, two-tiered silvacenosis (S_{sv1}) – 16%, terrain without vegetation – 36%.

The equation for the phytomelioration activity coefficient is as follows:

$$K_{FM} = \frac{S_{sv1\times b+S_r\times b+S_{p\times b}}}{s} \quad (14)$$

2010: pratocenosis (S_p) – 40%, ruderocenosis (S_r.) – 8%, single-tier silvacenosis (S_{sv1}) – 20%, terrain without vegetation – 32%.

The equation for the phytomelioration activity coefficient is as follows:

$$K_{FM} = \frac{S_{sv1\times b+S_r\times b+S_{p\times b}}}{s} \quad (15)$$

2000: pratocenosis (S_p) – 43%, ruderocenosis (S_r.) – 6%, single-tier silvacenosis (S_{sv1}) – 23%, frutocenosis (S_f) – 3%, terrain without vegetation – 25%.

The equation for the phytomelioration activity coefficient is as follows:

$$K_{FM} = \frac{S_{sv1\times b+S_f\times b+S_{p\times b+S_{r\times b}}}}{s} \quad (16)$$

1984: pratocenosis (S_p) – 46%, ruderocenosis (S_r.) – 5%, single-tier silvacenosis (S_{sv1}) – 25%, frutocenosis (S_f) – 6%, terrain without vegetation – 18%.

The equation for the phytomelioration activity coefficient is as follows:

$$K_{FM} = \frac{S_{sv1\times b+S_f\times b+S_{p\times b+S_{r\times b}}}}{s} \quad (17)$$

For a comprehensive calculation of the phytomelioration efficiency coefficient, an indicator b plays an important role, which takes into account the complexity of the effective impact of a particular plant cenosis. The following important indicators are taken into account: sea-

sonal phytomass, oxygen production, filtering properties due to habitat and type of vegetative cover, impact on microclimate, noise absorption and optical impact.

The average values of the points (b) of green mass (phytomeliorative cover) were used, as shown in **Table 1**.

Table 1. Mean values of green mass (b) (according to **Kucheryavyi, 2003**)

Type of phytocenosis	Green mass, (*b*)
Pratocenosis	0.7
Agrocenosis	1.0
Ruderocenosis	0.8
Frutocenosis	4.0
Pomolohocenosis	5.0
Streptocenosis	8.5
Single-tier silvacenosis	9.0

As a result of the calculations of phytomeliorative efficiency coefficients, the following results were obtained during the studied periods (see **Table 2**).

The calculations of the coefficients of phytomeliorative efficiency of the vegetation cover of the studied areas showed a clear dependence of the indicator decrease during the increase of the devastation area of the territory.

Differentiation of the dynamics of phytomeliorative efficiency coefficients for the studied periods revealed the following values: sinkhole No. 1 - 0.8; sinkhole No. 2 - 1.4; sinkhole No. 3 - 1.3; sinkhole No. 4 - 1.1.

Table 2. The value of phytomeliorative efficiency coefficients

Sinkhole No.	Year	The value of phytomeliorative efficiency coefficients, K_{FM}
1	2024	2.8
	2010	3.0
	2000	3.3
	1984	3.6
2	2024	3.5
	2010	3.8
	2000	4.2
	1984	4.9
3	2024	3.3
	2010	3.6
	2000	4.0
	1984	4.6
4	2024	3.0
	2010	3.2
	2000	3.5
	1984	4.1

The analysis of the presented tree-shrub and grass cover is as follows:

Tree-shrub species: English oak (*Quercus robur* L.) – Beech (Fagaceae), grey alder (*Alnus incana* (L.) Moench) – Birch (Betulaceae), silver birch (*Betula pendula* Roth.) – Birch (Betulaceae), aspen (*Populus tremula* L.) – Willow (Salicaceae), black locust (*Robinia pseudoacacia* L.) – Bean (Fabaceae), silver poplar (*Populus alba*) – Willow (Salicaceae), ash-leaved maple (*Acer negundo* L.) – Soapberry (Sapindaceae).

Herbaceous species: white clover (*Trifolium repens* L.) – Bean (Fabaceae), meadow fescue (*Lolium pratense* (Huds.) Darbysh.) – Grasses (Poaceae), smooth bromegrass (*Bromus inermi Leyss.*) – Grasses (Poaceae), meadow foxtail (*Alopecurus pratensis* L.) – Grasses (Poaceae), Kentucky bluegrass (*Poa pratensis* L.) – Grasses (Poaceae), timothy-grass (*Phleum praense* L.) – Grasses (Poaceae), sweet vernal grass (*Anthoxanthum odoratum* L.) – Grasses (Poaceae), bushgrass (*Calamagrostis epigejos* (L.)) – Grasses (Poaceae), couch grass (*Elymus repens* (L.) Gould) – Grasses (Poaceae), perennial ryegrass (*Lolium perenne* L.) – Grasses (Poaceae), spiny plumeless thistle (*Carduus acanthoides* L.) – Aster (Asteraceae), dandelion (*Taraxacum officinale* Wigg.) – Aster (Asteraceae), mugwort (*Artemisia vulgaris* L.) – Aster (Asteraceae), quaking sedge (*Carex brizoides* L.) – Sedges (Cyperaceae), broadleaf plantain (*Plantago major* L.) – Plantain (Plantaginaceae), wild carrot (*Daucus carota* L.) – Umbellifers (Apiaceae), silverweed (*Potentilla anserina* L.) – Rose (Rosaceae), common ragweed (*Ambrosia artemisiifolia* L.) – Aster (Asteraceae), spiny cocklebur (*Xanthium spinosum* L.) – Aster (Asteraceae), three-lobe beggarticks (*Bidens tripartita* L.) – Aster (Asteraceae), honey clover (*Melilotus albus* Medik.) – Bean (Fabaceae), peppergrass (*Lepidium ruderale* L.) – Mustards (Brassicaceae), common knotgrass (*Polygonum aviculare* L.) – Knotweed (Polygonaceae), curlycup gumweed (*Grindelia squarrosa Pursh.*) – Aster (Asteraceae), diffuse knapweed (*Centaurea diffusa* Lam.) – Aster (Asteraceae), yarrow (*Achillea millefolium* L.) – Aster (Asteraceae), giant sumpweed (*Iva xanthiifolia* Nutt.) – Aster (Asteraceae), Volga fescue (*Festuca valesiaca* A ex Gaudin) – Grasses (Poaceae), coltsfoot (*Tussilago farfara L.*) – Aster (Asteraceae) (Yeremenko, 2019).

Among the tree and shrub species, the largest representation of the families birch (Betulaceae) and Willow (Salicaceae) was found - 2 species in each, Beech (Fagaceae), Bean (Fabaceae), and Soapberry (Sapindaceae) - 1 species in each.

Among the herbaceous species, the following families were found: Aster (Asteraceae) - 11 species, Grasses (Poaceae) - 10 species, Bean (Fabaceae) - 1 species, Umbellifers (Apiaceae) - 1 species, Sedges (Cyperaceae) - 1 species, Plantain (Plantaginaceae) - 1 species, Rose (Rosaceae) - 1 species, Mustards (Brassicaceae) - 1 species, and Knotweed (Polygonaceae) - 1 species.

The analysis of the dynamics of territorial devastation growth from 1984 to 2024 was as follows: sinkhole No. 1 - 9.4; sinkhole No. 2 - 1.85; sinkhole No. 3 - 2.15; sinkhole No. 4 - 6.35.

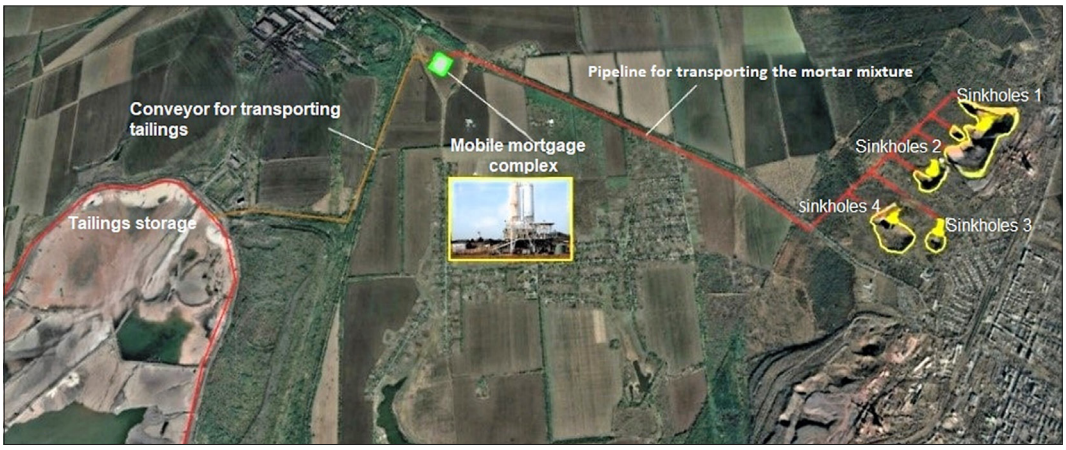

Figure 14. Scheme of backfill priority mine sinkholes (coordinates: 48.0668, 33.4052)

Table 3. Regression equations for predicting sinkhole area dynamics

Sinkhole No.	Dependence	Equation	R^2
1	Linear dependence	$y = 0.2186x - 402.66$	0.870
	Polynomial dependence	$y = 0.0003x^3 - 1.8969x^2 + 3812.6x - 3 \cdot 10^6$	0.990
2	Linear dependence	$y = 0.0508x - 95.332$	0.990
	Polynomial dependence	$y = -3 \cdot 10^{-5} x^3 + 0.1805x^2 - 361.15x + 240816$	0.990
3	Linear dependence	$y = 0.0661x - 130.52$	0.890
	Polynomial dependence	$y = -0.0001x^3 + 0.7061x^2 - 1411.9x + 940915$	0.970
4	Linear dependence	$y = 0.1882x - 366.92$	0.970
	Polynomial dependence	$y = -0.0002x^3 + 1.4483x^2 - 2898.8x + 2 \cdot 10^6$	0.997

Hence, the greatest intensity of sinkhole expansion is in sinkhole No. 1, the intensity of sinkhole No. 4 is somewhat lower, and as of the time of the field research, the intensity of sinkhole No. 3 is still significantly lower - 2.15 and sinkhole No. 2 - 1.85. However, given the ongoing active influence of both exogenous factors (wind and water erosion, landslides, rockslides) and endogenous factors (karst and suphosion processes), these indicators may increase, which will undoubtedly be a significant factor in increasing threats to the environment and the safety of the region's population. Therefore, it is important to implement a set of measures that would slow down and, in the long run, eliminate this complex of large-scale threats.

3.4. Technological recommendation for sinkhole remediation

Based on the results of phytomelioration assessment and analysis of sinkhole dynamics, a cemented paste backfilling technology was proposed to mitigate geotechnical risks and restore land stability. The conceptual scheme is shown in **Figure 14**. This approach ensures long-term sealing of voids and minimizes the surface impact of underground mining (**Hubina & Zaborovsky, 2022**). A tailing volume is taken from the dry or wetted areas of the tailing dump and transported by machinery to the loading point. These tailings, formed during ore concentration and metallurgical processing, typically contain fine fractions of iron oxides (Fe_2O_3), quartz, aluminosilicates, and residual amounts of magnetite, along with trace concentrations of industrially valuable components such as rare earth elements (REEs), vanadium, titanium, and phosphorus. Several studies have confirmed the economic potential of reprocessing such materials for secondary metal extraction or use in construction, agriculture, or cement production (**Hubina & Zaborovsky, 2022**). From the loading point, the tailings are delivered to a conveyor line, which transports them to a mobile filling complex. In the backfilling complex, the tailings are mixed with a combined binder (Portland cement, ground blast furnace granulated slag and fly ash from the thermal power plant) and water. In the mixer, the components of the paste filling are mixed to a paste consistency with a specified solid content, and the pase filling mixture is transported by a pressure pump through the laid pipeline network to the sinkholes, where they are gradually filled from the bottom of the sinkhole to the top (**Bazaluk et al., 2024; Petlovanyi & Sai, 2024**).

3.5. Analysis of changes in the cost of restoration of disturbed areas

The analysis of the dependence of the change in the sinkhole area during 1984-2024 showed that this rela-

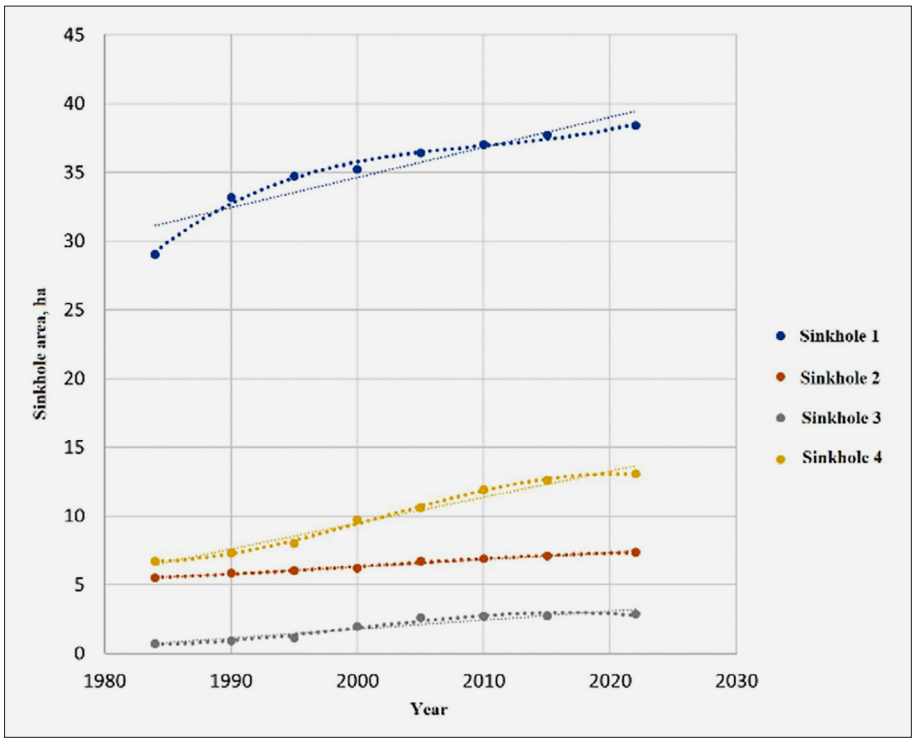

Figure 15. Dependence of sinkhole area change in time

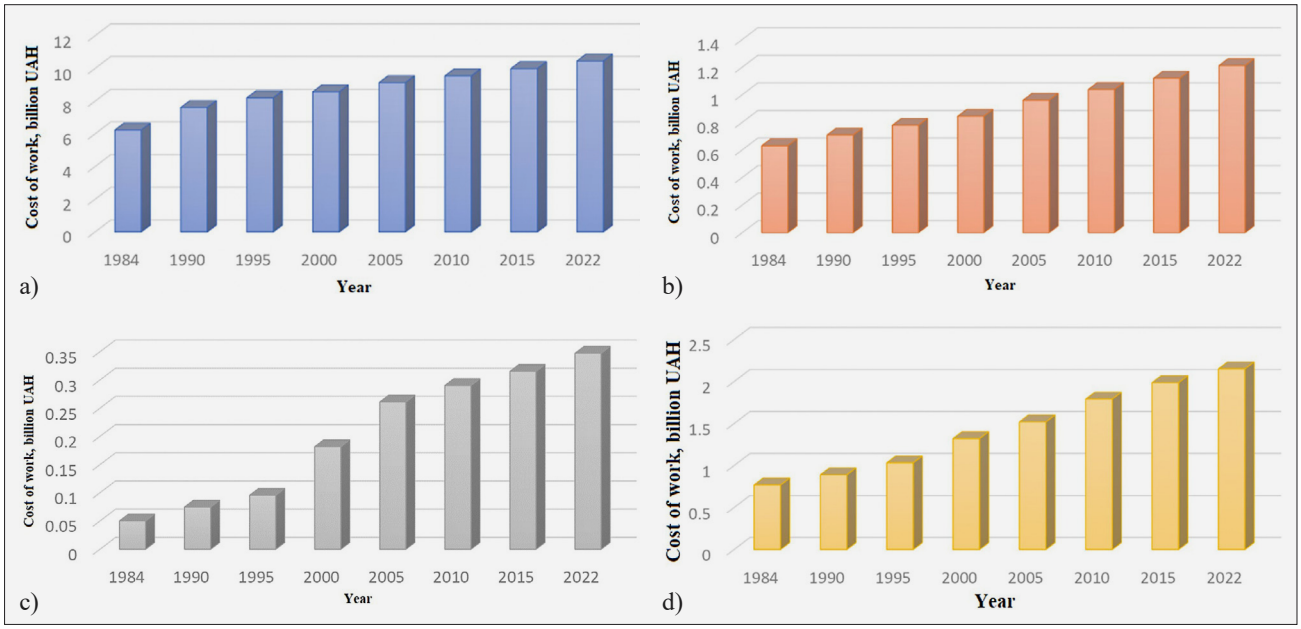

Figure 16. Dependence of the change in the cost of sinkhole filling on the time of its formation: a - sinkhole No. 1, b - sinkhole No. 2, c - sinkhole No. 3, d - sinkhole No. 4.

tionship is best described by a third-degree polynomial, as evidenced by the high values of the coefficient of determination. **Table 3** presents the equations obtained as a result of approximating the experimental data within the framework of the linear equation and the third-degree polynomial equation, and **Figure 15** shows the graphical dependence of the change in the sinkhole area over time.

Figure 16 shows that all but the largest sinkholes sharply increase in size between 1995 and 2005, which may indicate both the influence of some external factors (active rock mining, explosions, earthquakes) and the general dependence of sinkhole formation. Sinkhole 1 is also characterized by phases of sharp growth and deceleration of the sinkhole processes.

From source analysis, it follows that the average depth of such sinkholes ranges from 180 to 250 m (**Koptieva, 2021**). After calculating the volume of sinkholes and basing on the results of calculating the cost of their elimination (**Prozorro, 2023**), it was possible to estab-

lish the dependence of the change in the cost of such works on time.

It is obvious that delaying the start of work on the restoration of disturbed areas leads to a significant increase in their cost. In particular, the cost of eliminating sinkhole No. 3 over 38 years has increased almost 7 times - from UAH 50.2 million to UAH 347.2 million, while the cost of filling in sinkholes No. 2 and No. 4 will increase by 2 to 2.8 times, respectively. The cost of liquidation of the largest of the sinkholes, No. 1, will change the least, by 68% from UAH 6.2 billion to UAH 10.5 billion. These estimations were based on procurement data and budget reports retrieved from the Prozorro electronic system. Although no formal inflation-adjusted economic model was applied, the differences in values over time implicitly reflect inflation, currency devaluation, and changes in market conditions. This empirical trend clearly highlights the economic risks of postponing revitalization efforts. Obviously, backfilling of small sinkholes is the most economically feasible, as the depth of such sinkholes is actively growing over time along with their surface, which leads to a significant increase in investment in case of untimely liquidation.

While cemented paste backfilling shows promise in mitigating surface deformations and restoring geotechnical stability, its long-term ecological impact remains insufficiently explored. Future research should focus on evaluating the effectiveness of CPB in preserving natural landscapes, improving soil-plant interactions, and supporting biodiversity recovery in rehabilitated areas. Monitoring programs combining geotechnical, botanical, and remote sensing data will be essential to validate the sustainability of this remediation method under different environmental conditions.

4. Conclusions

The research on technogenic safety and revitalization of devastated landscapes in the Kryvyi Rih basin revealed an urgent need to implement comprehensive measures to restore the disturbed areas.

The analysis of the dynamics of phytomelioration efficiency coefficients (Kfm) for sinkholes No. 1, No. 2, No. 3, and No. 4 showed a gradual decrease in the efficiency of vegetation cover, which is a consequence of the growth of devastated areas. The highest values of Kfm were registered in 1984: 3.6, 4.9, 4.6, and 4.1, respectively, while in 2024 these values decreased to 2.8, 3.5, 3.3, and 3.0. The smallest decrease in the coefficient was observed for sinkhole No. 1 (0.8), while the largest decrease was registered for sinkhole No. 2 (1.4).

The analysis of the structure of the vegetation cover of the sinkhole zones revealed a predominance of species adapted to poor soils and a moderate level of phytomeliorative efficiency, which indicates the potential for natural restoration of the territories. Meanwhile, the dynamics of the expansion of sinkholes, confirmed by GIS observations, indicates a steady increase in the area of devastation and a corresponding decrease in Kfm, which emphasizes the need for timely intervention to accelerate revitalization processes.

The research substantiated the effectiveness of the cemented paste backfilling technology for the elimination of sinkholes, which is one of the priority areas for the revitalization of devastated areas. The proposed method enables the utilization of accumulated mining wastes and solving a number of engineering and environmental problems, including reduction of deformation processes, improvement of safety for the population and restoration of soil cover.

The analysis of the dynamics of changes in the area of sinkholes in 1984-2024 showed that their growth is best described by third-degree polynomial dependencies with high values of the coefficient of determination (up to 0.997). This indicates the nonlinear nature of the development of deformation processes. A particularly intensive increase in the area of failures was observed in the period 1995-2005. It has also been established that postponing revitalization works significantly increases their cost: in some cases, the costs increase by 2-7 times. Thus, timely intervention is not only environmentally sound, but also economically beneficial.

The research confirms the urgency and economic feasibility of introducing cemented paste filling technologies for the revitalization of devastated landscapes in the Kryvyi Rih basin. The timely implementation of the proposed measures will minimize anthropogenic risks, restore ecological balance and ensure sustainable development of the industrial region.

5. References

Agboola, O., Babatunde, D. E., Fayomi, O. S. I., Sadiku, E. R., Popoola, P., Moropeng, L., Yahaya, A., & Mamudu, O. A. (2020). A review on the impact of mining operation: Monitoring, assessment and management. Results in Engineering, 8, 100181. https://doi.org/10.1016/j.rineng.2020.100181

Batyr, Y., Lopatchenko, I., Aliieva, P., Akhmedova, O., Ruban, A., Stankevych, S., Zelenin, Y., & Kanakova, A. (2021). Environmental protection and public environmental policy in Ukraine. *Ukrainian Journal of Ecology, 11*(2), 346–348.

Bazaluk, O., Petlovanyi, M., Sai, K., Chebanov, M., & Lozynskyi, V. (2024). Comprehensive assessment of the earth's surface state disturbed by mining and ways to improve the situation: Case study of Kryvyi Rih Iron-ore Basin, Ukraine. Frontiers in Environmental Science, 12, Article 1480344. https://doi.org/10.3389/fenvs.2024.1480344

Bujok, P., Klempa, M., Slivka, V., Porzer, M., Němec, I., Šťastná, V., … Zdvořák, J. (2015). Remediation of the old ecological load in the protected area of the Morava River – Re-abandonment of oil and gas production wells. 30(1), 1–8. https://doi.org/10.17794/rgn.2015.1.4

Cabinet of Ministers of Ukraine. (2013). Resolution of the Cabinet of Ministers of Ukraine dated January 3, 2013 No.

22-r on the approval of the Concept of the National Program for Waste Management for 2013-2020. Retrieved from https://zakon.rada.gov.ua/laws/show/22-2013-%D1%80#Text (In Ukrainian)

Evtekhov, R. M., Koptieva, T. S., & Boyko, T. M. (2022). Fault-block tectonics and the consequences of deep ore mining in Kryvbas. Mining of Mineral Deposits, 16(3), 215–223. https://doi.org/10.33271/mining16.03.215

Gorman, M. R., & Dzombak, D. A. (2018). A review of sustainable mining and resource management: Transitioning from the life cycle of the mine to the life cycle of the mineral. Resources, Conservation & Recycling, 137, 281–291. https://doi.org/10.1016/j.resconrec.2018.06.001

Hren, L., Chebotarev, M., Ruban, A., Shvedun, V., Sysoieva, S., Stankevych, S., Smirnova, L., & Sokolov, A. (2021). The philosophy of environmental management: Evolution of the scientific conceptions. Ukrainian Journal of Ecology, 11(2), 378–381.

Hubina, V. H., & Zaborovsky, V. S. (2022). Priority technogenic mineral resources of iron ore mining and mineral processing plants of the Kryvyi Rih Basin. Proceedings of the 16th International Conference Monitoring of Geological Processes and Ecological Condition of the Environment, 1–5. https://doi.org/10.3997/2214-4609.2022580154

Kariuki, D. W., & Kuria, J. M. (2021). Coal – Key energy resource for the future in Kenya? A review. International Journal of Advanced Research, 3(1). https://doi.org/10.37284/ijar.3.1.319

Kazakov, V.L., Paranko, I.S., Smetana, M.H., Shipunova, V.O., Kotsyuruba, V.V., & Kalinichenko, O.O. (2005). Pryrodnycha heohrafiya Kryvbasu. Vydavnychyi dim. (In Ukrainian)

Koptieva, T. S. (2021). Altitudinal differentiation and diversity of mining landscapes of Kryvorizhzhia (Doctoral dissertation, Vinnytsia State Pedagogical University). *(In Ukrainian)*

Kryvbassproekt. (2011). General plan of the settlement. Explanatory note (2319/11365-MD.PZ.). Ministry of Industrial Policy of Ukraine, State Enterprise "State Institute for Design of Mining and Ore Processing Enterprises "Kryvbassproekt". Retrieved from https://data.gov.ua/dataset/7ecfe68e-cf5c-41b9-a004-c29bf0c7dd87/resource/7271335f-add7-4fce-bf0b-f058cc6ce66d/download/2319-11365-md-pz.pdf (In Ukrainian)

Kucheriavyy, V. P. (2003). Phytomelioration. Lviv: "Svit". 440 p. (In Ukrainian)

Loredo, J., Ordonez, A., & Alvarez, R. (2006). Environmental impact of toxic metals and metalloids from the Munon Cimero mercury-mining area (Asturias, Spain). Journal of Hazardous Materials, 136(3), 455–467. https://doi.org/10.1016/j.jhazmat.2006.01.048

Maiti, S. K., & Ahirwal, J. (2019). Chapter 3 - Ecological restoration of coal mine degraded lands: Topsoil management, pedogenesis, carbon sequestration, and mine pit limnology. In P. B. T. Phytomanagement of Polluted Sites (Ed.), Phytomanagement of Polluted Sites (pp. 83–111). Elsevier. https://doi.org/10.1016/B978-0-12-813912-7.00003-X

Neral, N., Kudelić, A., Maričić, A., & Mileusnić, M. (2023). Pottery technology through time: Archaeometry of pottery and clayey raw material from the multi-period site in eastern Croatia. Rudarsko-geološko-naftni zbornik, 38(2), 1–21. https://doi.org/10.17794/rgn.2023.2.1

Nouri Qarahasanlou, A., Khanzadeh, D., Shahabi, R. S., & Basiri, M. H. (2022). Introducing sustainable development and reviewing environmental sustainability in the mining industry. Rudarsko-geološko-naftni zbornik, 37(4), 91–108. https://doi.org/10.17794/rgn.2022.4.8

Pactwa, K., Woźniak, J., & Dudek, M. (2020). Coal mining waste in Poland in reference to circular economy principles. Fuel, 270, 117493. https://doi.org/10.1016/j.fuel.2020.117493

Petlovanyi, M., & Sai, K. (2024). Research into cemented paste backfill properties and options for its application: A case study from the Kryvyi Rih Iron-ore Basin, Ukraine. Mining of Mineral Deposits, 18(4), 162–179. https://doi.org/10.33271/mining18.04.162

Popovych, V., Bosak, P., Petlovanyi, M., Telak, O., Karabyn, V., & Pinder, V. (2021). Environmental safety of phytogenic fields formation on coal mines tailings. News of the National Academy of Sciences of the Republic of Kazakhstan, Series of Geology and Technical Sciences, 2(446), 129–136. https://doi.org/10.32014/2021.2518-170X.44

Popovych, V., Voloshchyshyn, A. I. (2019). Environmental impact of devastated landscapes of Volhynian Upland and Male Polissya (Ukraine). Ekologija ir aplinkos tyrimai, 75(3), 33–45. https://doi.org/10.5755/j01.erem.75.3.23323

Popovych, V., Voloshchyshyn, A., Lysyi, N., Petlovanyi, M., & Shuplat, T. (2024). Natural phytomelioration processes on rock dumps of abandoned coal mines (Ukraine). 39(5), 63–73. https://doi.org/10.17794/rgn.2024.5.4

Prozorro. (2023, June 8). Tender UA-2023-06-08-005416-a. Retrieved from https://prozorro.gov.ua/tender/UA-2023-06-08-005416-a (In Ukrainian)

Pukish, A., Mandryk, O., Arkhypova, L., Syrovets, S., & Hryniuk, D. (2024). Mathematical modeling of pollution of underground aquifers due to mining of minerals. *Mining of Mineral Deposits, 18*(3), 94–103. https://doi.org/10.33271/mining18.03.094

Serhiyenko, V. A., & Serhiyenko, A. A. (2022). Diabetes mellitus and congestive heart failure. Mizhnarodnij Endokrynologichnij Zhurnal, 18(1), 57–69. https://doi.org/10.22141/2224-0721.18.1.2022.1146

Skrobala, V., Popovych, V., & Pinder, V. (2020). Ecological patterns for vegetation cover formation in the mining waste dumps of the Lviv-Volyn coal basin. Mining of Mineral Deposits, 14(2), 119–127. https://doi.org/10.33271/mining14.02.119

Strömberg, B., & Banwart, S. (1994). Kinetic modelling of geochemical processes at the Aitik mining waste rock site in northern Sweden. Applied Geochemistry, 9(5), 583–595. https://doi.org/10.1016/0883-2927(94)90020-5

United Nations Framework Convention on Climate Change (UNFCCC). (2015). Paris Agreement. Retrieved from https://unfccc.int/process-and-meetings/the-paris-agreement/the-paris-agreement

Yeremenko, N. S. (2019). Syngenetic changes of ruderal vegetation of Kryvyi Rih. Ukrainian Botanical Journal, 76(1), 31-41. https://doi.org/10.15407/ukrbotj76.01.031 (In Ukrainian)

SAŽETAK

Industrijska metoda za ublažavanje površinskih devastacija i obnova strukture tla u bazenu Krivoga Roga

Studija istražuje kritična pitanja tehnogene sigurnosti i obnove devastiranih krajolika u bazenu Krivoga Roga, jednom od najvažnijih rudarskih područja Ukrajine. Istraživanje naglašava ekološke izazove uzrokovane intenzivnom rudarskom aktivnošću, uključujući stvaranje vrtača, degradaciju tla i gubitak bioraznolikosti, što je dodatno pogoršano klimatskim promjenama i erozijom. Analizom koeficijenata fitomelioracijske učinkovitosti (Kfm) studija procjenjuje učinkovitost vegetacijskoga pokrova, otkrivajući stalan pad od 1984. do 2024. zbog širenja devastiranih područja. Primjerice, vrijednosti Kfm za vrtaču br. 1 pale su s 3,6 na 2,8, a to upućuje na smanjenu ekološku otpornost. Ključni fokus istraživanja jest tehnologija ispunjavanja s cementiranom pastom, koja se koristi rudarskim otpadom za popunjavanje vrtača. Cilj je ove metode smanjiti devastirane površine, poboljšati javnu sigurnost i obnoviti strukturu tla, istovremeno reciklirajući industrijske nusproizvode. Korištenjem GIS-a i povijesnih podataka studija analizira dinamiku vrtača, identificirajući nelinearne obrasce povećanja, posebno u razdoblju od 1995. do 2005. Polinomski modeli (s R^2 do 0,997) učinkovito opisuju ove trendove. Ekonomska analiza ističe rastuće troškove odgađane revitalizacije, s povećanjem troškova do sedam puta tijekom 38 godina. Zaključeno je kako kombinacija tehnologije ispunjavanja i strategije fitomelioracije nudi održivo rješenje za obnovu krajolika Krivoga Roga usklađujući se s globalnim klimatskim ciljevima i regionalnim razvojnim potrebama. Rezultati ističu hitnu potrebu za provedbom predloženih mjera kako bi se osigurala ekološka stabilnost i dugoročne socioekonomske koristi.

Ključne riječi:
tehnogena sigurnost, revitalizacija krajolika, sanacija vrtača, koeficijent fitomelioracije, rekultivacija rudarskoga otpada

Author's contribution

Mykhailo Petlovanyi (PhD, Assistant) proposed and defined the idea of the scientific article, managed the field research, provided suggestions for interpretation of the results and graphical presentation of the data, and adjustment of the article. **Iryna Fediv** (PhD), **Vasyl Popovych** (Dr. Sci., Professor), **Taras Boyko** (PhD), **Kateryna Stepova** (PhD, Assistant), **Roman Konanets** (PhD) and **Nataliya Popovych** performed the field work, provided funding for the fieldwork, data collection and modelling, participated in the field research and analysis, graphically presented the data, and gave input into the discussion and conclusion sections.
All authors have read and agreed to the published version of the manuscript.